CORTEX 103 (2018) 224–239

Available online at www.sciencedirect.com

ScienceDirect

Journal homepage: www.elsevier.com/locate/cortex

Clinical neuroanatomy

Cross-talk connections underlying dorsal and ventral stream integration during hand actions

Sanja Budisavljevic [a,*], *Flavio Dell'Acqua* [b,c] *and Umberto Castiello* [a,d]

[a] *Department of General Psychology, University of Padova, Padova, Italy*
[b] *NatBrainLab, Department of Forensic and Neurodevelopmental Sciences, Institute of Psychiatry, Psychology and Neuroscience, King's College London, London, United Kingdom*
[c] *Sackler Institute for Translational Neurodevelopment, Institute of Psychiatry, Psychology and Neuroscience, King's College London, United Kingdom*
[d] *Centro Linceo Interdisciplinare, Accademia Nazionale dei Lincei, Roma, Italy*

ARTICLE INFO

Article history:
Received 25 August 2017
Reviewed 16 November 2017
Revised 15 January 2018
Accepted 21 February 2018
Action editor Georg Goldenberg
Published online 9 March 2018

Keywords:
Arcuate fasciculus
Dorsal stream
Skilled actions
Ventral stream
Vertical occipital fasciculus

ABSTRACT

According to the dual-stream theory, the processing of visual information is divided into a ventral pathway mediating object recognition, and a dorsal pathway supporting visuomotor control. Increasing evidence suggests that these streams are not independent, but where this dorsal-ventral stream integration occurs remains unknown. We explored the candidate white matter pathways linking dorsal and ventral visual streams in 30 right-handed participants performing object-oriented hand movements of varying complexity (reaching, grasping and lifting), using advanced diffusion imaging tractography based on the spherical deconvolution and kinematical analysis. We provided for the first time a direct evidence of cross-communication between dorsal and ventral visual streams in humans, through vertical occipital fasciculus and temporo-parietal fibers of the arcuate fasciculus during on-line control of grasping and lifting actions. We showed that individual differences in the microstructure of these cross-talk connections were associated with the variability of the arm deceleration, the grip opening and the grasp accuracy. This study suggests that hand kinematics, in skilled hand actions where high degree of online control is required, is related to the anatomy of the cross-talk networks between dorsal and ventral streams, bringing important insights to the dual-stream theory and the sensorimotor organization of hand actions.

1. Introduction

When we reach, grasp and lift an object, fast integration of sensory information is crucial for performing the movement successfully. According to a dual-stream theory, the processing of visual information is divided into a ventral 'perception' pathway extending to the inferotemporal cortex that mediates object recognition, and a dorsal 'action' pathway

* *Corresponding author*. University of Padova, Via Venezia 8, 35131, Padova, Italy.
E-mail address: sanja.budisavljevic@gmail.com (S. Budisavljevic).
https://doi.org/10.1016/j.cortex.2018.02.016

projecting to the posterior parietal cortex that supports visuomotor control (Goodale, 2014; Milner & Goodale, 2008; Rizzolatti & Matelli, 2003; Ungerleider & Mishkin, 1982). While a degree of functional specialization and segregation invariably exists between the two streams, information processed by the two networks must closely interact in everyday life, especially for more complex behavior such as skilled hand actions (Cloutman, 2013; Milner, 2017; van Polanen & Davare, 2015). Nevertheless, little attention has been paid to how, where, and when the dual streams interact.

Significant insights first emerged from anatomical tract tracing studies in monkeys, describing direct reciprocal interconnections between the two visual streams. For example, ventral inferior temporal area TE has strong bidirectional projections to the inferior parietal lobe (Zhong & Rockland, 2003) and prefrontal cortex (Borra, Ichinohe, Sato, Tanifuji, & Rockland, 2010; Gerbella, Belmalih, Borra, Rozzi, & Luppino, 2010), while the anterior intraparietal sulcus is interconnected to the superior and middle temporal gyri of the ventral stream (Borra et al., 2008). Similarly, diffusion magnetic resonance imaging (MRI) studies in humans reported white matter tracts between superior/middle temporal and inferior parietal regions (Budisavljevic et al., 2015; Catani et al., 2007, 2005) and between dorsal and ventral occipital visual areas (Yeatman, Rauschecker, & Wandell, 2013, 2014). Thus, anatomy points to inter-stream communication that could underlie integration between the two visual pathways. From a functional point of view, studies of the time course and laminar activation profiles in the monkey brain, showed that the two networks engage in a direct cross-talk at multiple stages, at least within the visual domain (Chen et al., 2007; Givre, Schroeder, & Arezzo, 1994; Oram & Perrett, 1996; Schroeder, Mehta, & Givre, 1998). Similarly, functional MRI studies in humans observed that the two streams are not independent, since they exhibit strong functional connectivity during object recognition (Freud, Rosenthal, Ganel, & Avidan, 2015; Sim, Helbig, Graf, & Kiefer, 2015) and likely communicate regarding the visual and motor dimensions relevant for the execution of hand actions (Bracci & Peelen, 2013; Fabbri, Stubbs, Cusack, & Culham, 2016; Konen & Kastner, 2008; Mahon, Kumar, & Almeida, 2013; Oosterhof, Wiggett, Diedrichsen, Tipper, & Downing, 2010).

Overall, evidence suggests that the integration between the two streams could occur at different levels, including i) shared target brain regions (e.g., prefrontal cortex), ii) feedback loops, and iii) by 'continuous cross-talk' at multiple stages and locations through direct lateral connections between the two streams (Cloutman, 2013). This integration might be especially important for more complex actions, when the dorsal stream needs to retrieve detailed information about object identity stored in the ventral stream areas, while the ventral stream receives up-to-date grasp-related information from dorsal areas to refine the object internal representation (van Polanen & Davare, 2015). Up to date, no research study has investigated the 'continuous cross-talk' possibility between the two streams. Our work aims to fill this gap by exploring the candidate cross-talk connections in humans and their role in skilled actions that are thought to require dorsal and ventral visual stream integration.

Based on the current neuroanatomical models of dual stream processing (Distler, Boussaoud, Desimone, & Ungerleider, 1993; Felleman & Van Essen, 1991; Ungerleider, Galkin, Desimone, & Gattass, 2008) we hypothesized that the vertical occipital fasciculus (VOF) and the posterior segment of the arcuate fasciculus (pAF), both connecting the lateral surfaces of the ventral and dorsal streams, enable the continuous cross-talk between the two visual streams (Fig. 1A). The VOF is the only major white matter pathway allowing the communication between dorsal and ventral visual maps with full hemifield representations (Takemura et al., 2016; Weiner, Yeatman, & Wandell, 2016; Yeatman et al., 2014, 2013). The VOF likely carries signals from the ventral regions that encode object properties such as form, identity, and color (Cohen et al., 2000; Malach et al., 1995; McKeefry & Zeki, 1997; Wade, Brewer, Rieger, & Wandell, 2002; Zeki et al., 1991) to dorsal regions that map spatial location to action plans (Fischer, Bulthoff, Logothetis, & Bartels, 2012; Merriam, Gardner, Movshon, & Heeger, 2013; Tootell et al., 1997). Parallel and anterior to the VOF, the neighbouring pAF is a temporo-parietal pathway intermingled within the arcuate fasciculus

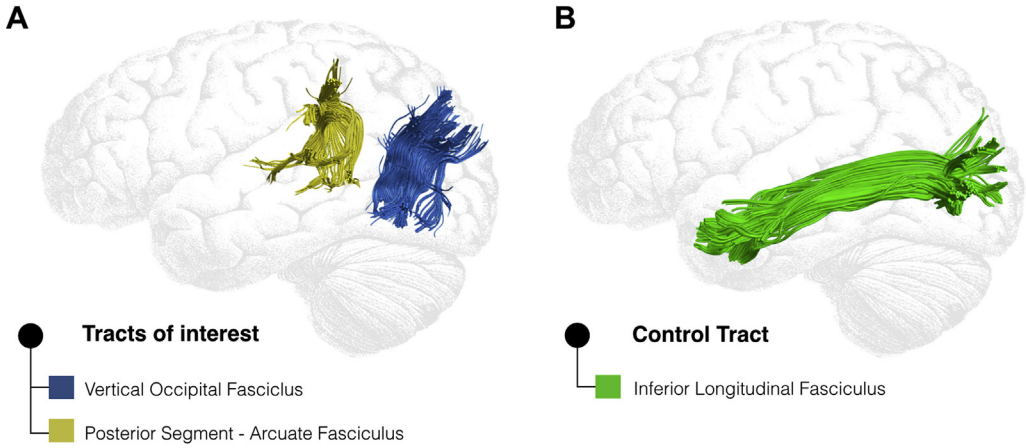

Fig. 1 – Descriptive example of A) the cross-talk connections (tracts of interest) including the VOF (in blue) and the pAF (in yellow); and B) the control tract, ILF in the left hemisphere (in green).

fibers, connecting the inferior parietal lobe with the superior and middle temporal gyri (Budisavljevic et al., 2015; Catani et al., 2007, 2005; Ramayya, Glasser, & Rilling, 2010; Thiebaut de Schotten, Cohen, Amemiya, Braga, & Dehaene, 2014). The pAF connections could represent part of a ventro-dorsal network of the extended dual-stream processing model (Rizzolatti & Matelli, 2003), which serves as an integration node and plays a role in both perception and action (Milner, 1997; Rizzolatti & Matelli, 2003; Shapiro, Hillstrom, & Husain, 2002; Singh-Curry & Husain, 2009).

In this study we tested the role of these cross-talk connections in hand actions of increasing complexity: i) simple reaching movements, which rely on the spatial information about the body and the target object, ii) reach-to-grasp movements (referred to as 'grasping'), which require additional sensorimotor processing of 3D intrinsic object properties, and lastly iii) reach-to-grasp-to-lift actions (referred to as 'lifting'), which compared to grasping also integrate non-visual object's weight information in order to scale fingertip forces accordingly. Diffusion imaging tractography based on the spherical deconvolution (SD) was chosen over the classical diffusion tensor model because it can better resolve the crossing fibers problem, affecting both the VOF and the pAF, and improve tractography reconstructions by reducing the presence of false negatives (Tournier, Calamante, Gadian, & Connelly, 2004; Dell'Acqua, Scifo, Rizzo, Catani, Simmons, & Scotti, 2010; Dell'Acqua, Simmons, Williams, & Catani, 2013). The VOF and the pAF were dissected in 30 right-handed healthy participants, whose hand kinematics was separately recorded for reaching, grasping and lifting movements. In order to test the specificity of our findings, we also dissected a control tract – the left inferior longitudinal fasciculus (ILF) (Fig. 1B). This ventral temporo-occipital bundle, connecting visual areas to the amygdala and the hippocampus (Catani, Jones, Donato, & ffytche, 2003), plays a role in a variety of visual functions, including visual perception (ffytche, 2008; ffytche & Catani, 2005), visual memory (Ross, 2008), and face recognition (Fox, Iaria, & Barton, 2008). The hindrance modulated orientational anisotropy (HMOA) was used as a measure of white matter microstructure, representing a tract-specific index, and better reflecting the microstructural organization (e.g., myelination, axonal density, axon diameter and fiber dispersion) than the traditional voxel-specific diffusion indices (e.g., fractional anisotropy) (Dell'Acqua et al., 2010, 2013).

Increasing task complexity may require an increased contribution of cortical processing carried along the ventral visual stream and transfer of object-related information between ventral and dorsal streams. Thus, we hypothesized that the nature of the task would modulate the correlation between visuomotor behavior and cross-talk white matter microstructure. Associations between the cross-talk connections and the hand kinematics should be observed during grasping and lifting movements where more detailed (ventral) information about the object is needed, compared to reaching actions that rely predominantly on the dorsal stream. It should be noted that this is the first explorative study to test the 'continuous cross-talk' hypothesis in humans, and it was not designed to confirm or falsify specific predictions on the nature of expected correlations. We could though expect that the arm deceleration phase, which depends on visual feedback and involves sensorimotor adjustments for an efficient and accurate grasping and lifting of the object, together with specific measures concerned with the formation of the grasp, would be significantly associated with the anatomy of the lateral cross-talk connections.

2. Materials and methods

2.1. Participants

A sex and age-balanced sample of 30 healthy participants (13 males; mean age 24.6 ± 2.8, age range: 20–31 years) was recruited. All participants were right-handed according to the Edinburgh Handedness Inventory (Oldfield, 1971). No history of neurological and psychiatric disorders was present in the study sample. All participants gave informed written consent in accordance with the ethics approval by the Institutional Review Board at the University of Padova, in accordance with the Declaration of Helsinki (Sixth revision, 2008).

2.2. Behavioral experiment

2.2.1. Task and stimulus

Participants were requested to perform three tasks: i) a reaching task, in which they were asked to perform a movement toward the stimulus and touch the stimulus frontal surface with their knuckles, maintaining the hand in a closed fist, ii) a reach-to-grasp task (referred to as 'grasping'), in which they were asked to reach toward and grasp the stimulus with a precision grip (using an index finger and a thumb), and iii) a reach-to-grasp-to-lift task (referred to as 'lifting'), in which they reached toward and grasped the stimulus with a precision grip in order to move the object to an empty container (Fig. 2). Importantly, for lifting movements only the first 'reach-to-grasp' part was kinematically analyzed. The fist's posture was chosen as to minimize the distal involvement. Participants fixated the target object during all actions. The stimulus consisted of a small spherical object (2 cm in diameter) that would naturally be grasped with a precision grip. The size of the target object was kept the same, in order to maintain the same physical setting for the three tasks. All participants were explicitly asked to use a precision grip for grasping and lifting tasks. Trials in which the participants did not comply with the task or did not fixate the stimulus were not included in the analysis.

2.2.2. Procedure

Each participant sat on a height-adjustable chair in front of a table (900 × 900 mm) with the elbow and wrist resting on the table surface and the right hand in a designated start position. The hand was pronated with the palm resting on a pad (60 × 70 mm), shaped to allow for a comfortable and repeatable posture of all digits, i.e., slightly flexed at the metacarpal and proximal interphalangeal joints. The starting pad was attached 90 mm away from the edge of the table surface. The object was placed on a platform located at a distance of 300 mm between the platform and the sagittal plane of the hand's starting position on the right side of the table (Fig. 2).

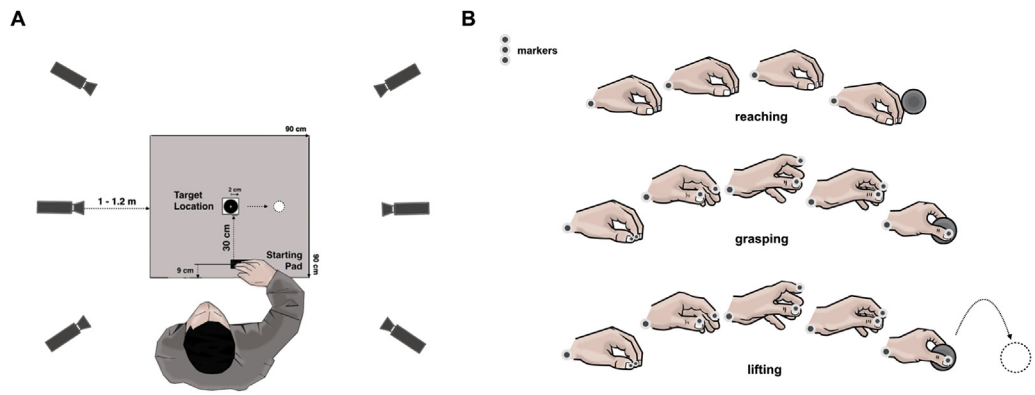

Fig. 2 – (A) Descriptive example of the experimental set up showing designated start position, target location, container location (white circle) and infrared cameras position. (B) Schematic drawing representing reaching, grasping and lifting movements.

2.2.3. *Kinematics recording*

A 3D-Optoelectronic SMART-D system (Bioengineering Technology and Systems, BTS) was used to track the kinematics of the participant's right upper limb. Three light-weight infrared reflective markers (.25 mm in diameter; B|T|S|) were taped to the following points: (i) thumb (ulnar side of the nail); (ii) index finger (radial side of the nail); and (iii) wrist (dorsodistal aspect of the radial styloid process). Six video cameras (sampling rate 140 Hz) detecting the markers were placed in a semicircle at a distance of 1–1.2 m from the table. The camera position, roll angle, zoom, focus, threshold, and brightness were calibrated and adjusted to optimize marker tracking, followed by static and dynamic calibration. For the static calibration, a three-axes frame of five markers at known distances from each other was placed in the middle of the table. For the dynamic calibration, a three-marker wand was moved throughout the workspace of interest for 60s. The spatial resolution of the recording system was .3 mm over the field of view. The standard deviation of the reconstruction error was below .2 mm for the x-, y-, and z-axes.

2.2.4. *Data processing*

Following data collection, each trial was individually checked for correct marker identification and the SMART-D Tracker software package (B|T|S|) was used to provide a 3-D reconstruction of the marker positions as a function of time. The data were then filtered using a finite impulse response linear filter (transition band = 1 Hz, sharpening variable = 2, cut-off frequency = 10 Hz; D'Amico & Ferrigno, 1990, 1992). Movement onset was defined as the time at which the tangential velocity of the wrist marker crossed a threshold (5 mm/sec) and remained above it for longer than 500 msec. For the grasping and lifting tasks the end of movement was defined as the time at which the hand made contact with the stimulus and quantified as the time at which the hand opening velocity crossed a threshold (−5 mm/sec) after reaching its minimum value and remained above it for longer than 500 msec. For the reaching task the end of movement was defined as the time at which the hand made contact with the stimulus and quantified as the time at which the wrist velocity crossed a threshold (5 mm/sec) after reaching its minimum value and remained above it for longer than 500 msec. For each of the three tasks, 12 trials were administered in a randomized order and the following kinematic 'reach' parameters were extracted using a custom protocol run in Matlab 2014b (The 4 MathWorks, Natick, MA, USA): the time interval between the movement onset and the end of movement (Movement Time), the time at which the tangential velocity of the wrist was maximum from the movement onset (Time to Peak Wrist Velocity), the time at which the acceleration of the wrist was maximum from the movement onset (Time to Peak Acceleration), the time at which the deceleration of the wrist was maximum from the movement onset (Time to Peak Deceleration). For grasping and lifting tasks additional 'grasp' kinematics was assessed, namely the time at which the distance between the thumb and index finger was maximum, between the movement onset and the hand contact time (Time to Maximum Grip Aperture) and its amplitude (Amplitude of Maximum Grip Aperture) the standard deviation of the Amplitude of Maximum Grip Aperture (Variability of the Maximum Grip Aperture) – a measure used to characterize the uncertainty or perceptual and/or motor inconsistency (i.e., accuracy) of the grasp formation (Flindall, Doan, & Gonzalez, 2014); and the time and amplitude of the maximum opening and closing grip velocity.

2.3. *MRI data acquisition*

Diffusion imaging data was acquired using a Siemens Avanto 1.5T scanner housed in Padova University Hospital with actively shielded magnetic field gradients (maximum amplitude 45 mT/m^{-1}). The body coil was used for RF transmission, and an 8-channel head coil for signal reception. Protocol consisted of a localizer scan, followed by a single-shot, spin-echo, EPI sequence with the following parameters: TR = 8500, TE = 97, FOV = 307.2 × 307.2, matrix size = 128 × 128, 60 slices (no gaps) with isotropic (2.4 × 2.4 × 2.4 mm^3) voxels. The maximum diffusion weighting was 2000 sec/mm^2, and at each slice location 7 images were acquired with no diffusion gradients applied (b = 0 sec/mm^2), together with 64 diffusion-weighted images in which gradient directions were uniformly distributed in space and repeated 3 times, in order to increase signal to noise ratio (SNR). Gains and scaling factors were kept constant between acquisitions. Scanning lasted approximately 30 min.

2.4. Correction of motion and eddy current distortion, and estimation of the fiber orientation distribution (FOD)

Each subject's raw image data were examined before proceeding on to further analyses to detect any outliers in the data, including signal drop-outs, poor signal-to-noise ratio, and image artifacts such as ghosts. Any subject whose raw data contained volumes with significant image quality issues was removed from further analyses. The remaining 30 participants were processed as follows.

DWI datasets were concatenated and corrected for subject motion and geometrical distortions using ExplorDTI (http://www.exploredti.com; Leemans, Jeurissen, Sijbers, & Jones, 2009). SD (Tournier, Calamante, & Connelly, 2007, 2004; Dell'Acqua, Rizzo, Scifo, Clarke, Scotti, & Fazio, 2007) approach was chosen to estimate multiple orientations in voxels containing different populations of crossing fibers. SD was calculated applying the damped version of the Richardson-Lucy algorithm with a fiber response parameter $\alpha = 1.5$, 200 algorithm iterations and η=.15 and $\nu = 15$ as threshold and geometrical regularization parameters (Dell'Acqua et al., 2010). An example of the recovered FOD profiles obtained with these settings is provided in the Supplementary Material (Figure S1). Fiber orientation estimates were obtained by selecting the orientation corresponding to the peaks (local maxima) of the FOD profiles. To exclude spurious local maxima, we applied both an absolute and a relative threshold on the FOD amplitude (Dell'Acqua et al., 2013). The first "absolute" threshold corresponding to a HMOA threshold of .015 was used to exclude intrinsically small local maxima due to noise or partial volume effects with isotropic tissue. This threshold was set to select only the major fiber orientation components and exclude low amplitude spurious FOD components obtained from gray matter and cerebro-spinal fluid isotropic voxels. The second "relative" threshold of 5% of the maximum amplitude of the FOD was applied to remove remaining unreliable local maxima with values greater than the absolute threshold but still significantly smaller than the main fiber orientation (Dell'Acqua et al., 2013).

2.5. Tractography algorithm

Whole brain tractography was performed selecting every brain voxel with at least one fiber orientation as a seed voxel. From these voxels, and for each fiber orientation, streamlines were propagated using a modified Euler integration with a step size of 1 mm. When entering a region with crossing white matter bundles, the algorithm followed the orientation vector of the least curvature. Streamlines were halted when a voxel without fiber orientation was reached or when the curvature between two steps exceeded a threshold of 45°. All SD and tractography processing was performed using StarTrack, a freely available Matlab software toolbox developed by one of the authors (F.D. NatBrainLab, King's College London), and based on the methods described in Dell'Acqua et al. (2013).

2.6. Tractography dissections of dorsal-ventral white matter connections

To visualize fibre tracts and quantify tract-specific measures we used TrackVis software (http://www.trackvis.org; Wang, Benner, Sorensen, & Wedeen, 2007). Examples of tractography reconstructions in representative subjects are shown in Fig. 3.

2.6.1. VOF

We used a one region of interest (ROI) drawn on consecutive axial slices around a cluster of occipital voxels posterior to the arcuate fibers and immediately lateral to the ILF, with a vertically oriented principal diffusion direction (color-coded in blue). We retained the candidate fibers within the occipital lobe that are primarily vertical and removed fibers that belonged to the pAF. This method has been previously described in Yeatman et al. (2013, 2014).

2.6.2. pAF

We used a two regions of interest (ROIs) approach to isolate the pAF, according to a dissection method previously described in Catani, Jones, and ffytche (2005, 2007) and Budisavljevic et al. (2015). Two separate ROIs were manually delineated on the fractional anisotropy (FA) maps of each subject in the inferior parietal lobule and the posterior temporal region of each hemisphere. All streamlines passing through these two ROIs were considered to belong to the pAF.

2.6.3. ILF

We used a two ROIs approach to dissect the ILF that acted as a control tract, according to a method previously described in Catani et al. (2003). The first ROI was manually placed around the white matter of the anterior temporal lobe, while the second ROI was defined around the white matter of the occipital lobe, with both ROIs drawn on consecutive axial FA slices.

Lastly, although novel multi fiber methods like SD improve the visualization of anatomical connections not visible with traditional diffusion tensor methods, SD can produce more false positives. To control for this bias we visually inspected all the tracts, in addition to using an absolute threshold based on HMOA, as explained previously.

2.7. Statistical analysis

Statistical analysis was performed using SPSS software (Version 21) (SPSS, Chicago, IL). Gaussian distribution was confirmed for kinematic and tractography HMOA variables using the Shapiro–Wilk test (α-level: $p < .05$) (Shapiro & Wilk, 1965) allowing the use of parametric statistics. The mean value for each kinematic parameter of interest was determined based on 12 individual observations for each participant. Repeated measures ANOVA analyses were performed separately for each kinematic measurement (i.e., total movement time, time of peak velocity, acceleration, deceleration) to examine kinematical differences between the three movement tasks (i.e., the fixed factor). Paired-samples *t*-tests were conducted for comparing grasp-specific measures of grasping versus lifting movements. Post hoc comparisons for specific tasks were considered

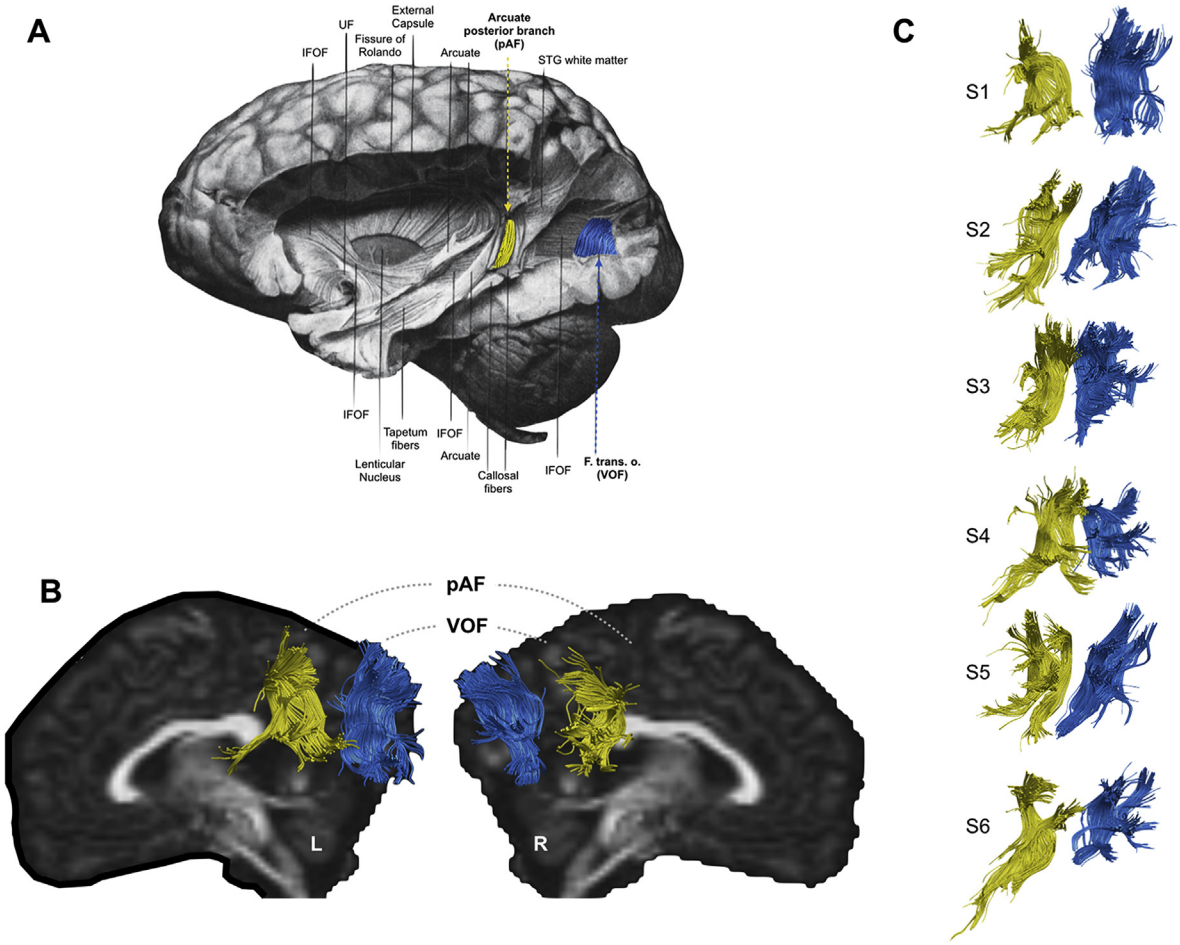

Fig. 3 – A) pAF (yellow) and VOF (blue) tractography reconstructions overlaid on a post-mortem dissection figure by Curran (1909). The course of the fasciculus is viewed from the lateral aspect of the hemisphere, B) example of tractography reconstructions of the pAF and VOF in the left and the right hemisphere in a representative single subject, C) inter-individual variability of the pAF and VOF in the left hemisphere for six additional subjects (S1–S6). Abbreviations: pAF, posterior segment of the arcuate fasciculus; VOF, vertical occipital fasciculus; IFOF, inferior fronto-occipital fasciculus; UF, uncinate fasciculus; STG, superior temporal gyrus; F.trans.o., posterior part of the fasciculus transversus occipitalis (VOF), most of which has been removed in image A) to show a large window through which the IFOF can be observed.

statistically significant if they survived Bonferroni correction for multiple comparisons (α-level: $p < .05$).

The mean HMOA was calculated for each tract in each subject, defined as the absolute amplitude of each lobe of the FOD, and representing a quantitative index of the degree of tract anisotropy. HMOA was chosen over voxel-based FA as it is considered to be a tract-specific index highly sensitive to axonal myelination, fiber diameter and axonal density (Dell'Acqua et al., 2013). The main difference between FA and HMOA is that FA is a traditional voxel-based metrics providing an average measure of anisotropy of the entire voxel derived from fitting the data according to the diffusion tensor model. On the contrary, HMOA is a new tract-specific metrics based on the SD approach. The main advantages of HMOA are: i) resolving partial volume contamination of different white matter tracts crossing within the same voxel or brain region, and ii) providing a distinct and therefore a more "true" tract-specific quantification of anisotropy and microstructural organization along each white matter tract (i.e., if two fibers are crossing the same voxel, two distinct and independent HMOA values are assigned to each tract) (Dell'Acqua et al., 2013). However, in order to test our a priori assumed higher sensitivity of the tract-specific HMOA index to detect significant associations, compared to the traditional voxel-based FA measure, we have performed a posteriori correlation analysis also on the FA measures of our tracts of interest.

Pearson bivariate correlation analysis was used to detect the strength of the correlation between the tract-specific HMOA measure and the kinematic markers of reaching, grasping and lifting movements. We employed a false discovery rate (FDR) correction (Benjamini & Hochberg, 1995) for 104 comparisons using the q-value of .05 for significant results (FDR $p < .05$), which treated 26 different kinematic parameters and four HMOA values for four different fiber bundles (VOF and pAF, bilaterally) as instances of multiple testing. As a posteriori analysis, we extracted and performed the correlation analysis also on the control tract – the left ILF, to test the specificity of our findings.

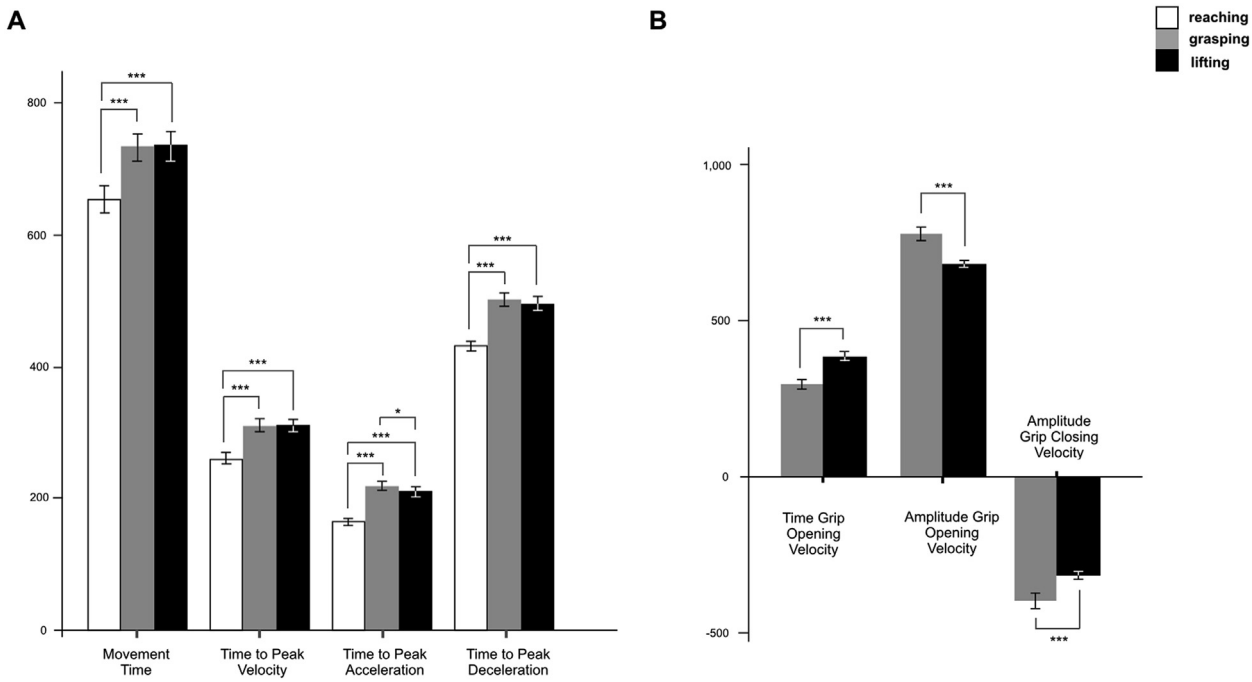

Fig. 4 – Kinematical markers showing statistically significant differences between (A) reaching, grasping and lifting movements and (B) between grasping and lifting movements. Errors bars: 95% CI. ***$p < .001$, *$p < .05$.

3. Results

3.1. *Behavioral results*

Movement times and the mean kinematic values of reaching, grasping and lifting actions are shown in Table S1 of the Supplementary Material. Although we have used a mixed sex group for the study, there was no significant effect of sex on the kinematic measures (all $p > .066$). A one-way repeated measures analysis of variance (ANOVA) indicated significant differences in reach kinematics between the three tasks for the total movement time (F (2, 28) = 130.088, $p < .0001$), time to peak velocity (F (2, 28) = 96.552, $p < .0001$), time to peak acceleration (F (2, 28) = 146.793, $p < .0001$) and time to peak deceleration (F (2, 28) = 75.716, $p < .0001$). Post-hoc comparisons (Fig. 4A) showed that movement duration was shorter for reaching than for grasping (t (29) = −16.415, $p < .0001$) and lifting (t (29) = −13.035, $p < .0001$). Also, time to peak velocity, acceleration and deceleration was reached earlier for reaching than for grasping (t_{VEL} (29) = −13.987, $p < .0001$; t_{ACCEL} (29) = −17.436, $p < .0001$; t_{DECEL} (29) = −11.328, $p < .0001$) and lifting (t_{VEL} (29) = −13.279, $p < .0001$; t_{ACCEL} (29) = −17.199, $p < .0001$; t_{DECEL} (29) = −12.298, $p < .0001$). Time to peak acceleration was reached significantly earlier (t (29) = 2.666, $p = .012$) for lifting compared to grasping movement (Fig. 4A).

Regarding the grasp kinematics (Fig. 4B), the time of maximum grip opening velocity was reached earlier for grasping compared to lifting (t (29) = −9.091, $p < .0001$), while the amplitudes of the maximum grip opening (t (29) = 10.343, $p < .0001$) and grip closing velocity (t (29) = −6.848, $p < .0001$) were significantly higher for grasping compared to lifting. The amplitude of the maximum grip aperture was not significantly different between grasping and lifting tasks (t (29) = −1.191, $p = .243$). This parameter is rather stable and the changes in grip aperture usually occur due to changes in object size, which in our tasks was identical. However, the variability of the maximum grip aperture was significantly lower for lifting compared to grasping (t (29) = 9.327, $p < .0001$), suggesting that grasping for lifting task was implemented more precisely and accurately than grasping the object when no subsequent action was requested.

3.2. *Relating inter-individual differences in movement kinematics to the anatomy of the cross-talk connections*

Tractography results for the VOF and the pAF (Fig. 3) revealed that these dorsal-ventral networks showed statistically significant associations between their microstructural integrity, indexed by HMOA, and the kinematics of the grasping (for VOF) and lifting movements (for VOF and pAF), but not for the reaching actions (Fig. 5; Table S2 of the Supplementary Material).

Since these pathways lie in close proximity to each other, it is important to mention that their tissue properties, in terms of HMOA, were highly correlated between the right VOF and the right ($r = .593$, $p < .0001$) and left pAF ($r = .629$, $p < .0001$); however the left VOF was independent of the left and right pAF ($p > .096$) but significantly correlated with its right counterpart ($r = .617$, $p = .0003$). Furthermore, just like for the kinematic measures, there was no effect of sex on the HMOA tract measures (all $p > .564$), hence the correlation analyses were done on a mixed sex group.

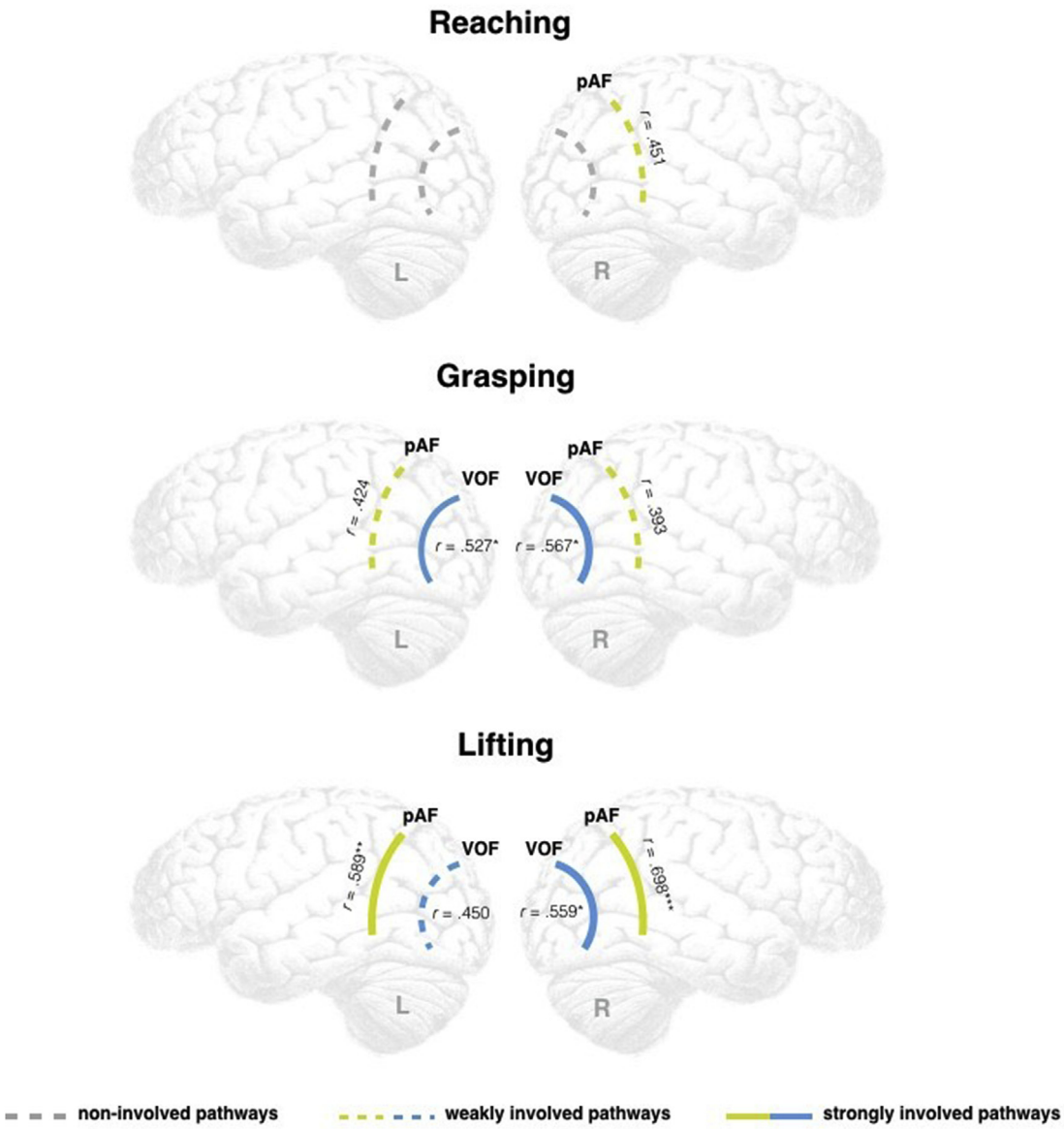

Fig. 5 – Graphical overview of the correlation analyses between HMOA and the kinematics of reaching, grasping and lifting movements. Dashed gray lines indicate that no associations were found (non-involved pathways), colored dashed lines denote an association was found but it did not survive the FDR correction (weakly involved pathways), while colored solid lines signify strong associations (strongly involved pathways) that survived the FDR correction. For VOF, correlations with the amplitude of the maximum opening grip velocity are shown, except for the left VOF and the variability of the maximum grip aperture in grasping task; for the pAF, correlations with the time to peak deceleration are shown. Abbreviations: pAF, posterior segment of the arcuate fasciculus; VOF, vertical occipital fasciculus. Significance codes represent FDR adjusted *p*-values: *$p < .05$; **$p < .01$; ***$p < .001$.

Our a posteriori analysis based on the FA measure revealed similar trends in data, reflected in weak associations with the kinematics of grasping (VOF) and kinematics of lifting (VOF and pAF), which failed to reach significance after the FDR correction ($p > .025$). Although the indices of FA and HMOA were significantly correlated in all the tracts, i.e., the left ($r = .464$, $p = .010$) and right pAF ($r = .559$, $p = .001$), the left ($r = .540$, $p = .002$) and right VOF ($r = .551$, $p = .002$), as hypothesized the tract-specific HMOA measure seemed more sensitive to detect the associations with the kinematic markers compared to the classical voxel-based FA measure. Lastly, we observed no significant correlations for HMOA or FA values of our control tract – the left ILF (Table S2 of the Supplementary Material) and kinematic markers, even before performing the FDR correction (all $p > .070$). The inter-individual variability of the HMOA measure of the left ILF was higher (SD = .013, or 14.7% of the mean value) than that of the bilateral VOF and pAF (all SD < .007, or up to 13.2% of the mean value), thus the lack of correlation shown in the control tract could not be due to the lack of variation.

3.2.1. *Kinematics and the VOF*

Our results showed strong association of the bilateral VOF with the grasp phase of both grasping and lifting actions, indicating a contribution of the left VOF in the transfer of accuracy information for the formation of hand choreography during grasping, and a contribution of the right VOF in the grip opening phase during both grasping and lifting actions (Fig. 6; Table S2 of the Supplementary Material).

HMOA of the left VOF was correlated with the level of variability of the maximum grip aperture. For the grasping movements higher HMOA corresponded to greater variability of the maximum grip aperture ($r = .527$, $p = .002$) and, consequently, to less accuracy. This relationship was not found for lifting movements ($r = .194$, $p = .302$). The difference between the correlations of HMOA and the time of maximum grip aperture for the two movements was not significant ($z = 1.532$, $p = .125$). The possible reason for the lack of significant correlation between HMOA and the maximum grip aperture for the lifting task might lie in the fact that the variability of the maximum grip aperture for lifting was significantly lower compared to grasping – thus not variable enough to detect differences between the subjects. Lastly, although the right VOF was not significantly related to the variability of the maximum grip aperture during grasping, this correlation was not significantly different from the one observed for the same movement within the left VOF ($z = 1.453$, $p = .146$).

Secondly, higher HMOA of the right VOF corresponded to higher amplitude of the maximum opening grip velocity for both grasping ($r = .567$, $p = .001$) and lifting actions ($r = .559$, $p = .001$). Although correlations involving the left VOF failed to survive the FDR correction (grasping: $r = .425$, $p = .019$, lifting: $r = .450$, $p = .012$) (Fig. 6), there was no significant difference between the correlations of the left and right VOF with the amplitude of maximum opening grip velocity during grasping ($z = 1.012$, $p = .311$) or lifting ($z = -.779$, $p = .435$). Thus, it is likely that the bilateral VOF is associated with the grip opening phase as the hand is approaching the target object in order to either grasp or lift it.

3.2.2. *Kinematics and the pAF*

We observed a statistically significant relationship between the bilateral pAF and the transport (reach) component of lifting actions (Fig. 6; Table S2 of the Supplementary Material). In particular, higher HMOA of the bilateral pAF was associated with a later time to peak deceleration in lifting movements (left pAF: $r = .589$, $p < .001$; right pAF: $r = .698$, $p < .0001$), a kinematic marker indexing a careful arm deceleration phase for guiding the hand to a stable final fingers' positioning. Although we found correlations between the time to peak

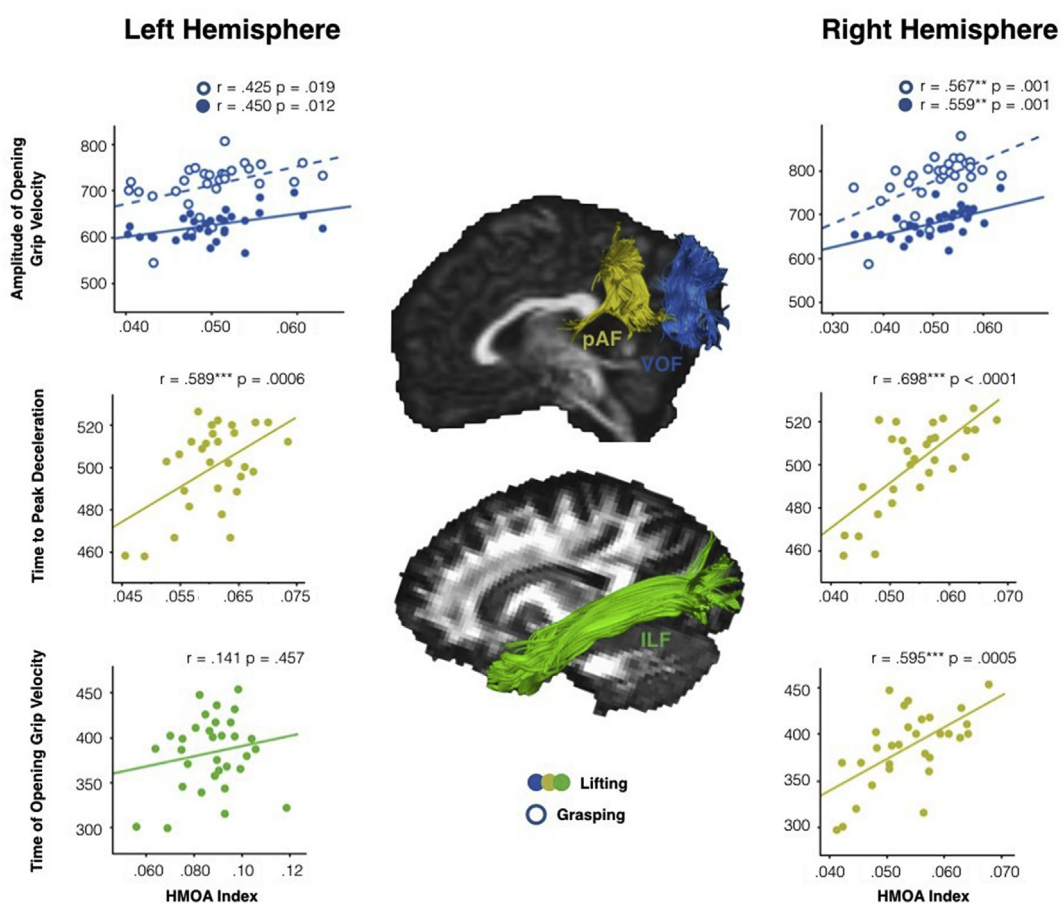

Fig. 6 – Correlation plots showing the associations between the bilateral VOF (in blue), the bilateral pAF (in yellow), and the left ILF control tract (in green) in terms of HMOA and the kinematics of grasping and lifting movements. Significance codes show corresponding FDR adjusted *p*-values at '*' $p < .001$ and '**' $p < .01$.**

deceleration and the right pAF in reaching ($r = .451$, $p = .012$) and the bilateral pAF in grasping (left pAF: $r = .424$, $p = .019$; right pAF: $r = .393$, $p = .032$) movements, these correlations did not survive the FDR correction but they were not statistically different from the above-mentioned significant correlations for the lifting kinematics (all $p > .123$).

The grasp-specific kinematics was also significantly associated with the pAF during lifting, but not during grasping movements. Higher HMOA of the right pAF corresponded to longer time of the maximum opening grip velocity during lifting movements ($r = .595$, $p < .001$). Although the correlation with the left pAF failed to survive the FDR correction ($r = .431$, $p = .018$), there was no significant difference between the correlations of the left and right pAF ($z = -1.011$, $p = .312$) and the time of the maximum opening grip velocity, pointing to the fact that bilateral pAF plays a specific role for lifting actions given that the correlations for the grasping condition were significantly different from the lifting ones (for the right pAF: $z = -3.773$, $p = .0001$; for the left pAF: $z = -2.478$, $p = .013$).

In sum, although the bilateral pAF could be related to the arm deceleration phase for all the considered movements, it seems to be particularly associated with the timing of the opening grip aperture when the object needs to be lifted and not solely grasped.

4. Discussion

Despite the apparent segregation, neurophysiological, neuroimaging and lesion studies indicate that dorsal and ventral visual streams need to communicate in everyday life for successful execution of complex behaviors (Cloutman, 2013; De Haan & Cowey, 2011; Goodale, 2014; Milner, 2017; Schenk & McIntosh, 2009; van Polanen & Davare, 2015). Our study tried to answer the question of whether and how these two visual streams interact with one another to support visually guided skilled hand actions. We explored whether the performance of hand actions characterized by different levels of complexity, namely reaching, grasping and lifting, is modulated by the anatomy of cross-talk connections between the dorsal and ventral visual streams.

We demonstrate, for the first time, that lateral occipital and temporo-parietal white matter pathways mediate the cross-talk between the two visual streams in order to support skilled hand actions. We suggest that the VOF and the pAF are at the basis of the anatomical coupling between dorsal and ventral regions, and that the nature (i.e., complexity) of the task modulates the correlation between visuomotor behavior and their white matter microstructure. We observed that the anterior pAF was significantly associated with the arm deceleration phase of lifting movements. It is during the deceleration phase that an efficient control and the execution of small trajectory adjustments occur as the hand approaches the target object. Furthermore significant associations with the cross-talk connections were also found at the level of the grasp component with specific reference to the speed (pAF) and amplitude (VOF) adopted to reach the maximum grip aperture and the associated variability (VOF) indexing accuracy of the grasp. These parameters are vital for a successful grasp given that it is immediately after the time maximum grip aperture is reached that the honing phase of the fingers upon the object starts. This phase must allow for enough time to determine and implement contact points and minimize variability.

Our findings confirmed that a close collaboration exists between the ventral and dorsal visual streams in skilled actions, in line with the functional neuroimaging literature. For example, an involvement of the ventral stream was shown for processing grasp-related properties such as object size, shape, and weight (Cavina-Pratesi, Goodale, & Culham, 2007; Gallivan, Cant, Goodale, & Flanagan, 2014; Grill-Spector, Kushnir, Edelman, Itzchak, & Malach, 1998; Monaco et al., 2014), while object-selective responses were observed in dorsal stream regions (Fang & He, 2005; Grill-Spector, Kushnir, Hendler, & Malach, 2000; James, Humphrey, Gati, Menon, & Goodale, 2002; Konen & Kastner, 2008; Vinberg & Grill-Spector, 2008). Similarities were also noted between the representations of the viewed actions in the ventral and dorsal visual streams (Bracci & Peelen, 2013; Fabbri et al., 2016; Konen & Kastner, 2008; Mahon et al., 2013; Oosterhof et al., 2010; Roth & Zohary, 2015). There seems to be no absolute distinction between the two streams, and the linear hierarchical dual stream model has been recently modified towards a more interconnected network model (De Haan & Cowey, 2011). Thus, despite their functional specialization, our findings corroborate the notion that significant transfer of information exists between the two visual streams, enabling both to contribute to complex visuomotor behavior.

However, in a simple action context such as reaching (i.e., transport of the arm in space to the location of a target object), after correction for multiple comparisons no significant correlation between the anatomy of the considered cross-talk connections and kinematics was observed. This finding is consistent with the notion that the dorsal 'action' stream mediates the visual control of reaching actions (Milner & Goodale, 2008; Rizzolatti & Matelli, 2003; Ungerleider & Mishkin, 1982). In this respect, reaching activates the dorsal stream regions in functional MRI studies (Cavina-Pratesi et al., 2010; Filimon, Nelson, Huang, & Sereno, 2009; Prado et al., 2005) and it becomes selectively disrupted by transcranial magnetic stimulation over the posterior parietal cortex (Desmurget et al., 1999) and in patients with severe optic ataxia whose dorsal stream is damaged (Buxbaum & Coslett, 1998; Gréa et al., 2002; Pisella et al., 2000; Rossetti et al., 2005). Our group has recently showed that dorsal white matter networks, such as fronto-parietal (Budisavljevic et al., 2016) and premotor pathways (Budisavljevic et al., 2017), significantly modulate the kinematics of reaching actions (see also Catani et al., 2017, for newly described intra-parietal connections that could also underly reaching movements). Nevertheless, it should be acknowledged that the inter-individual variability of the time to peak deceleration for reaching (unlike other reaching measures) was lower than for grasping and lifting actions, which could potentially reflect the observed lack of correlation.

4.1. Relating the kinematics of grasping and lifting to the anatomy of the VOF

Individual differences in the microstructure of the bilateral VOF were significantly associated with the variability of grasp-specific kinematics, i.e., the level of variability during grip formation for grasping, and the grip opening phase during both grasping and lifting actions.

Higher HMOA of the left VOF corresponded to higher variability of the grasp aperture during grasping task, while higher HMOA of the right VOF corresponded to higher amplitudes of the opening grip velocity during both grasping and lifting, i.e., faster opening of the hand up to maximum grip aperture. In other words, it seems that VOF transfers information relevant to the unfolding of the hand opening as the hand reaches the maximum grip aperture. Maximum grip aperture is the key kinematical parameter indexing the beginning of a hand closure (Jeannerod, 1984), and it is scaled mainly depending on the visual availability of objects and their intrinsic visual properties such as size and shape. The computation of these visual object properties is crucial for successful hand preshaping in grasping movements (Castiello, 2005), and when visual feedback is not available exaggerated opening of the hands occurs (Hesse, Miller, & Buckingham, 2016; Jakobson & Goodale, 1991).

Also, the variability of the maximum grip aperture, commonly used as an index of grasp accuracy and transport error (Flindall et al., 2014), was significantly associated with the anatomy of the VOF. Higher HMOA of the left VOF was associated with greater and more variable grip apertures. Kinematical studies showed that more variable and less accurate grip apertures, expected to occur when reaching faster, are often compensated with bigger opening of the hands (Wing, Turton, & Fraser, 1986). Similarly, in the present study the wider opening of the hand gives increased tolerance for positioning errors just prior to contact, and improves the chances of the hand encompassing the object before collision. We may speculate that subjects who had higher HMOA of the VOF had faster transfer of information between dorsal and ventral streams, leading to bigger and more variable grip apertures. Support for this suggestion comes from the assumption that an increase in HMOA reflects an increase in myelination level and axonal density, leading to faster signal conduction time (Dell'Acqua et al., 2010), possibly bringing a faster and greater fingers' opening. This is in line with a recent study showing that higher speed of visual information processing is associated with a higher HMOA of the fronto-parietal white matter networks (Chechlacz, Gillebert, Vangkilde, Petersen, & Humphrey, 2015). It must be said, however, that it is difficult to interpret differences in HMOA in a linear fashion since HMOA also increases with decreasing axonal radius and radial diffusivity (Dell'Acqua et al., 2010, 2013), possibly due to decreased myelination.

Thus, the VOF supports the transfer of object-related properties necessary for efficient grasp formation by allowing the communication between ventral regions that process intrinsic object properties and dorsal regions that map spatial location to action plans (Takemura et al., 2016; but see Freud, Plaut, & Behrmann, 2016 for dorsal stream in object perception). This is in line with studies showing a crucial role of the VOF fibers in the visual shape processing (Lee Masson, Wallraven, & Petit, 2017) and the ventral stream cortical areas in processing object size during grasping (Hesse et al., 2016; Schenk, 2012) – explaining why patients with optic ataxia and dorsal stream damage are able to use object size for grasping (Cavina-Pratesi, Ietswaart, Humphreys, Lestou, & Milner, 2010). Furthermore, recent evidence suggests that perceptual features, processed by the occipital ventral stream areas, are used as priors by the dorsal visuomotor stream to specify goal-directed grasping actions and are activated earlier in time than dorsal regions involved in specifying action plans (Zimmermann, Verhagen, de Lange, & Toni, 2016).

It is argued that formation of the grasp is planned to take into account not only the perceived visual characteristics of the object, but also internalized information based on the past experience about the likely accuracy of the reaching component (Wing et al., 1986), processed by the ventral stream regions. Thus, the VOF fibers may support object-directed skilled actions by fine-tuning the opening of the hand in order to decrease transport errors and accomplish an efficient and accurate grasp of a target object.

4.2. Relating the kinematics of lifting to the anatomy of the pAF

The pAF fibers connect the cortical nodes of a ventro-dorsal network (Rizzolatti & Matelli, 2003), e.g., the inferior parietal lobe and the superior temporal regions that play a crucial role in both perception and action, especially for skilled object use (Binkofski & Buxbaum, 2013; Iacoboni et al., 2001; Martin et al., 2016; Milner, 1997; Rizzolatti & Matelli, 2003; Shapiro et al., 2002; Singh-Curry & Husain, 2009). The parietal terminations of the bilateral pAF were often specifically implicated in lifting actions: i) the left intraparietal sulcus in reactive online adjustments of grip force for lifting (Dafotakis, Sparing, Eickhoff, Fink, & Nowak, 2008), and ii) the right inferior parietal lobe in updating of predictive force scaling (Jenmalm, Schmitz, Forssberg, & Ehrsson, 2006), corrective reactions and updating of memory representations of object's weight (Schmitz, Jenmalm, Ehrsson, & Forssberg, 2005) and dynamic object manipulation and anticipatory coordination of grip and load forces maintaining grasp stability during lifts (Ehrsson, Fagergren, Johansson, & Forssberg, 2003). This is why it was not surprising that the pAF connections were strongly associated with the kinematics of the lifting actions.

Lifting actions require an additional factor – object's weight, to be incorporated into the motor plan and used to calculate the necessary grip and lift fingertip forces (Nowak, Glasauer, & Hermsdörfer, 2013). Properties such as weight are not directly specified in the visual information, but are part of the object's identity for which both perception and memory are important (Kentridge, 2014). In other words, weight is relevant to skilled object manipulation and is estimated based on stored knowledge and more conceptual identity information processed by the ventral stream. Evidence that expectations about the object's weight are represented in the ventral stream regions (Gallivan et al., 2014) and that visual information from the ventral pathway can influence weight estimations during

lifting (Brenner & Smeets, 1996; Jackson & Shaw, 2000), may explain the strong correlations of lifting kinematics with the cross-talk pAF (and VOF) fibers. Furthermore, people can adjust their lifting movements online after a sudden visible change in object's weight despite a short time frame (Brouwer, Georgiou, Glover, & Castiello, 2006). It is argued that this online adjustment, thought to rely on the dorsal stream, is influenced by visual cues about weight information processed by the ventral stream. Our findings corroborate the notion that although weight might be processed at the level of the ventral perceptual stream, this information could be made readily available to the visuomotor dorsal stream for online control through direct cross-talk connections.

More specifically, we found that the bilateral pAF fibers were significantly related to movement deceleration, which reflects the control phase during which comparisons between motor commands and sensory feedback occur and any necessary corrections to the original movement plan are made (Paulignan, MacKenzie, Marteniuk, & Jeannerod, 1990, 1991). Participants with higher HMOA of the bilateral pAF spent less time decelerating towards the target object during lifting, possibly implying faster transfer of object-related information, and less corrections made to the original movement plan. It is possible that the pAF, just like its cortical endpoint, the inferior parietal lobe (Schmitz et al., 2005; de Lange, 2006; Jenmalm et al., 2006), is part of a neural circuit involved in fast corrective responses triggered in lifts, monitoring a sensory mismatch and updating sensorimotor memories related to weight.

Previous research showed that movement deceleration affects the finger opening phase prior to contact, and suggested that the demands for precise control gradually increase when the fingers are almost at contact with the object (Chieffi & Gentilucci, 1993; Corradini, Gentilucci, Leo, & Rizzolatti, 1992; Lemon, Johansson, & Westling, 1995; Paulignan, Jeannerod, MacKenzie, & Marteniuk, 1991). This is reconcilable with our finding that the grip opening phase, i.e., the speed at which the hand was opened while approaching the target object before the lift, was also strongly associated with the pAF fibers. Higher microstructural organization of the right pAF corresponded to later time to maximum opening grip velocity. Longer time to reach maximum grip velocity may serve to extend the time window within which contact points can be established more precisely and firmly. During lifting it is necessary to carefully control finger positioning and the applied forces in order to avoid the tilting or falling of the target object (Lukos, Ansuini, & Santello, 2007). To do this, participants need to coordinate the 'braking' phase of the arm (i.e., deceleration phase) as to accompany the hand toward the object with the gradual opening of the fingers. The relationship between pAF fibers and the grip formation is in line with studies noting a crucial role of the human intraparietal sulcus in hand preshaping (Davare, Andres, Clerget, Thonnard, & Olivier, 2007; Tunik, Frey, & Grafton, 2005). These two kinematical features, arm deceleration and hand opening phase mark the on-line control processes (Glover, 2004). The dual role of the pAF in grip formation and arm deceleration reflects the prominent finding in the functional literature that the anterior intraparietal sulcus of the inferior parietal lobe has two main roles: i) the integration of intrinsic object properties, such as size and shape into a motor plan, and ii) the updating of grasp formation by online detection and correction of errors in motor execution (Dafotakis et al., 2008; Rice, Tunik, & Grafton, 2006; Tunik et al., 2005). We suggest that the pAF fibers are important in integrating visuomotor-specific information from the dorsal stream with the object-relevant information from the ventral stream in order to control the on-line movement trajectory and the grip formation during skilled hand actions such as lifting.

4.3. *Further implications*

As mentioned above, object weight is part of a high-level, non-visual object property that requires an elaborate conceptual processing. The fact that lifting actions were significantly related to the more anterior cross-talk pAF connections is in line with observations that the object's conceptual encoding occurs more in the anterior ventral areas, whereas the posterior ventral regions might respond more to specific visual properties, both in the monkey (Goda, Tachibana, Okazawa, & Komatsu, 2014) and human (Peelen & Caramazza, 2012) brains. This notion is further supported by the evidence that the anterior areas in the ventral stream process weight representations (Gallivan et al., 2014). Moreover, conceptual aspects of actions requiring knowledge of skilled object use were previously associated with the cortical terminations of the pAF fibers, the inferior parietal lobe (Binkofski & Buxbaum, 2013; Martin et al., 2016) and the superior temporal regions (Martin et al., 2016). Consistent with these observations we suggest that the anterior cross-talk connections, i.e., the pAF, might be specialized for higher-level, dynamic object-use representations (object weight). Instead, the posterior cross-talk VOF fibers might be more involved in visual representation of objects and crucial for grasp formation according to properties such as size, shape, and orientation in both grasping and lifting movements.

5. Conclusions

This is the first explorative study to demonstrate that the cross-talk between dorsal and ventral visual streams is supported by the vertical occipital (VOF) and temporo-parietal (pAF) white matter fibers. We observed a direct relationship between the anatomy of these bilateral cross-talk connections and dominant hand kinematics of skilled actions (i.e., grasping and lifting) requiring a high degree of online control. These pathways played an important role during the arm deceleration phase and the specification of a key parameter for a successful grasp, i.e., maximum grip aperture. However, the cross-talk integration is not the only form of communication between the dual processing streams, and important contributions from top-down feedback connections or additional common target brain areas should not be underestimated. We hope that future studies, combining multimodal approaches with larger data cohorts, will bring additional insights into the neural basis of dorsal-ventral stream integration.

Conflict of interest

None declared.

Acknowledgements

This work was supported by the Progetto Strategico, Università di Padova (N. 2010XPMFW4) to Umberto Castiello. We would like to thank NeMo laboratory (http://nemolaboratory.com) for helpful comments on the manuscript.

Supplementary data

Supplementary data related to this article can be found at https://doi.org/10.1016/j.cortex.2018.02.016.

REFERENCES

Benjamini, Y., & Hochberg, Y. (1995). Controlling the false discovery rate: A practical and powerful approach to multiple testing. *Journal of the Royal Statistical Society Series B (Methodological), 57*(1), 289–300.

Binkofski, F., & Buxbaum, L. J. (2013). Two action systems in the human brain. *Brain and Language, 127*(2), 222–229.

Borra, E., Belmalih, A., Calzavara, R., Gerbella, M., Murata, A., Rozzi, S., & Luppino, G. (2008). Cortical connections of the macaque anteriorintraparietal (AIP) area. *Cerebral Cortex, 18*(5), 1094–1111.

Borra, E., Ichinohe, N., Sato, T., Tanifuji, M., & Rockland, K. S. (2010). Cortical connections to area TE in monkey: Hybrid modular and distributed organization. *Cerebral Cortex, 20*(2), 257–270.

Bracci, S., & Peelen, M. V. (2013). Body and object effectors: The organization of object representations in high-level visual cortex reflects body-object interactions. *The Journal of Neuroscience, 33*(46), 18247–18258.

Brenner, E., & Smeets, J. B. (1996). Size illusion influences how we lift but not how we grasp an object. *Experimental Brain Research, 111*(3), 473–476.

Brouwer, A. M., Georgiou, I., Glover, S., & Castiello, U. (2006). Adjusting reach to lift movements to sudden visible changes in target's weight. *Experimental Brain Research, 173*(4), 629–636.

Budisavljevic, S., Dell'Acqua, F., Djordjilovic, V., Miotto, D., Motta, R., & Castiello, U. (2017). The role of the frontal aslant tract and premotor connections in visually guided hand movements. *Neuroimage, 146*, 419–428.

Budisavljevic, S., Dell'Acqua, F., Rijsdijk, F. V., Kane, F., Picchioni, M., McGuire, P., et al. (2015). Age-related differences and heritability of the perisylvian language networks. *The Journal of Neuroscience, 35*(37), 12625–12634.

Budisavljevic, S., Dell'Acqua, F., Zanatto, D., Begliomini, C., Miotto, D., Motta, R., et al. (2016). Asymmetry and structure of the fronto-parietal networks underlie visuomotor processing in humans. *Cerebral Cortex, 27*(2), 1532–1544.

Buxbaum, L. J., & Coslett, H. B. (1998). Spatio-motor representations in reaching: Evidence for subtypes of optic ataxia. *Cognitive Neuropsychology, 15*(3), 279–312.

Castiello, U. (2005). The neuroscience of grasping. *Nature Reviews Neuroscience, 6*(9), 726–736.

Catani, M., Allin, M. P., Husain, M., Pugliese, L., Mesulam, M. M., Murray, R. M., et al. (2007). Symmetries in human brain language pathways correlate with verbal recall. *Proceedings of the National Academy of Sciences USA, 104*(43), 17163–17168.

Catani, M., Jones, D. K., Donato, R., & ffytche, D. H. (2003). Occipito-temporal connection in the human brain. *Brain, 126*, 2093–2107.

Catani, M., Jones, D. K., & ffytche, D. H. (2005). Perisylvian language networks of the human brain. *Annals of Neurology, 57*(1), 8–16.

Catani, M., Robertsson, N., Beyh, A., Huynh, V., de Santiago Requejo, F., Howells, H., et al. (2017). Short parietal lobe connections of the human and monkey brain. *Cortex, 97*, 339–357.

Cavina-Pratesi, C., Goodale, M. A., & Culham, J. C. (2007). FMRI reveals a dissociation between grasping and perceiving the size of real 3D objects. *Plos One, 2*(5), e424.

Cavina-Pratesi, C., Ietswaart, M., Humphreys, G. W., Lestou, V., & Milner, A. D. (2010). Impaired grasping in a patient with optic ataxia: Primary visuomotor deficit or secondary consequence of misreaching? *Neuropsychologia, 48*(1), 226–234.

Cavina-Pratesi, C., Monaco, S., Fattori, P., Galletti, C., McAdam, T. D., Quinlan, D. J., et al. (2010). Functional magnetic resonance imaging reveals the neural substrates of arm transport and grip formation in reach-to-grasp actions in humans. *The Journal of Neuroscience, 30*(31), 10306–10323.

Chechlacz, M., Gillebert, C. R., Vangkilde, S. A., Petersen, A., & Humphrey, G. W. (2015). Structural variability within frontoparietal networks and individual differences in attentional functions: An approach using the theory of visual attention. *The Journal of Neuroscience, 35*(30), 10647–10658.

Chen, C. M., Lakatos, P., Shah, A. S., Mehta, A. D., Givre, S. J., Javitt, D. C., et al. (2007). Functional anatomy and interaction of fast and slow visual pathways in macaque monkeys. *Cerebral Cortex, 17*(7), 1561–1569.

Chieffi, S., & Gentilucci, M. (1993). Coordination between the transport and the grasp components during prehension movements. *Experimental Brain Research, 94*(3), 471–477.

Cloutman, L. L. (2013). Interaction between dorsal and ventral processing streams: Where, when and how? *Brain and Language, 127*(2), 251–263.

Cohen, L., Dehaene, S., Naccache, L., Lehericy, S., Dehaene-Lambertz, G., Henaff, M. A., et al. (2000). The visual word form area: Spatial and temporal characterization of an initial stage of reading in normal subjects and posterior split-brain patients. *Brain, 123*(Pt 2), 291–307.

Corradini, M. L., Gentilucci, M., Leo, T., & Rizzolatti, G. (1992). Motor control of voluntary arm movements. Kinematic and modelling study. *Biological Cybernetics, 67*(4), 347–360.

Curran, E. J. (1909). A new association fiber tract in the cerebrum. With remarks on the fiber tract dissection method of studying the brain. *Journal of Comparative Neurology, 19*(6), 645–656.

Dafotakis, M., Sparing, R., Eickhoff, S. B., Fink, G. R., & Nowak, D. A. (2008). On the role of the ventral premotor cortex and anterior intraparietal area for predictive and reactive scaling of grip force. *Brain Research, 1228*, 73–80.

Davare, M., Andres, M., Clerget, E., Thonnard, J. L., & Olivier, E. (2007). Temporal dissociation between hand shaping and grip force scaling in the anterior intraparietal area. *The Journal of Neuroscience, 27*(15), 3974–3980.

De Haan, E. H., & Cowey, A. (2011). On the usefulness of 'what' and 'where' pathways in vision. *Trends in Cognitive Sciences, 15*(10), 460–466.

Dell'Acqua, F., Rizzo, G., Scifo, P., Clarke, R. A., Scotti, G., & Fazio, F. (2007). A model-based deconvolution approach to solve fiber crossing in diffusion-weighted MR imaging. *IEEE Transactions on Biomedical Engineering, 54*(3), 462–472.

Dell'Acqua, F., Scifo, P., Rizzo, G., Catani, M., Simmons, A., Scotti, G., et al. (2010). A modified damped Richardson-Lucy algorithm to reduce isotropic background effects in spherical deconvolution. *Neuroimage, 49*(2), 1446–1458.
Dell'Acqua, F., Simmons, A., Williams, S. C., & Catani, M. (2013). Can spherical deconvolution provide more information that fiber orientations? Hindrance modulated orientational anisotropy, a true-tract specific index to characterize white matter diffusion. *Human Brain Mapping, 34*(10), 2464–2483.
Desmurget, M., Epstein, C. M., Turner, R. S., Prablanc, C., Alexander, G. E., & Grafton, S. T. (1999). Role of the posterior parietal cortex in updating reaching movements to a visual target. *Nature Neuroscience, 2*(6), 563–567.
Distler, C., Boussaoud, D., Desimone, R., & Ungerleider, L. G. (1993). Cortical connections of inferior temporal area TEO in macaque monkeys. *Journal of Comparative Neurology, 334*(1), 125–150.
D'Amico, M., & Ferrigno, G. (1990). Technique for evaluation of derivates from noisy biomechanical displacement data using model-based bandwidth-selection procedure. *Medical and Biological Engineering and Computing, 28*(5), 407–415.
D'Amico, M., & Ferrigno, G. (1992). Comparison between the more recent techniques for smoothing and derivative assessment in biomechanics. *Medical and Biological Engineering and Computing, 30*(2), 193–204.
Ehrsson, H. H., Fagergren, A., Johansson, R. S., & Forssberg, H. (2003). Evidence for the involvement of the posterior parietal cortex in coordination of fingertip forces for grasp stability in manipulation. *Journal of Neurophysiology, 90*(5), 2978–2986.
Fabbri, S., Stubbs, K. M., Cusack, R., & Culham, J. C. (2016). Disentagling representations of object and grasp properties in the human brain. *The Journal of Neuroscience, 36*(29), 7648–7662.
Fang, F., & He, S. (2005). Cortical responses to invisible objects in the human dorsal and ventral pathways. *Nature Neuroscience, 8*(10), 1380–1385.
Felleman, D. J., & Van Essen, D. C. (1991). Distributed hierarchical processing in the primate cerebral cortex. *Cerebral Cortex, 1*(1), 1–47.
ffytche, D. H., & Catani, M. (2005). Beyond localization: From hodology to function. *Philosophical Transactions of the Royal Society of London B Biological Sciences, 360*, 767–779.
ffytche, D. H. (2008). The hodology of hallucinations. *Cortex, 44*, 1067–1083.
Filimon, F., Nelson, J. D., Huang, R. S., & Sereno, M. I. (2009). Multiple parietal reach regions in humans: Cortical representations for visual and proprioceptive feedback during on-line reaching. *The Journal of Neuroscience, 29*(9), 2961–2971.
Fischer, E., Bulthoff, H. H., Logothetis, N. K., & Bartels, A. (2012). Human areas V3A and V6 compensate for self-induced planar visual motion. *Neuron, 73*(6), 1228–1240.
Flindall, J. W., Doan, J. B., & Gonzalez, C. L. (2014). Manual asymmetries in the kinematics of a reach-to-grasp action. *Laterality, 19*(4), 489–507.
Fox, C. J., Iaria, G., & Barton, J. J. S. (2008). Disconnection in prosopagnosia and face processing. *Cortex, 44*, 996–1009.
Freud, E., Plaut, D. C., & Behrmann, M. (2016). 'What' is happening in the dorsal visual pathway. *Trends in Cognitive Sciences, 20*(10), 773–784.
Freud, E., Rosenthal, G., Ganel, T., & Avidan, G. (2015). Sensitivity to object impossibility in the human visual cortex: Evidence from functional connectivity. *Journal of Cognitive Neuroscience, 27*(5), 1029–1043.
Gallivan, J. P., Cant, J. S., Goodale, M. A., & Flanagan, J. R. (2014). Representation of object weight in human ventral visual cortex. *Current Biology, 24*(16), 1866–1873.
Gerbella, M., Belmalih, A., Borra, E., Rozzi, S., & Luppino, G. (2010). Cortical connections of the macaque caudal ventrolateral prefrontal areas 45A and 45B. *Cerebral Cortex, 20*(1), 141–168.
Givre, S. J., Schroeder, C. E., & Arezzo, J. C. (1994). Contribution of extrastriate area V4 to the surface-recorded flash VEP in the awake macaque. *Vision Research, 34*(4), 415–428.
Glover, S. (2004). Separate visual representations in the planning and control of action. *The Behavioral and Brain Sciences, 27*(1), 3–24.
Goda, N., Tachibana, A., Okazawa, G., & Komatsu, H. (2014). Representation of the material properties of objects in the visual cortex of nonhuman primates. *The Journal of Neuroscience, 34*(7), 2660–2673.
Goodale, M. A. (2014). How (and why) the visual control of action differs from visual perception. *Proceedings of the Royal Society B: Biological Sciences, 281*(1785), 20140337.
Gréa, H., Pisella, L., Rossetti, Y., Desmurget, M., Tilikete, C., Grafton, S., et al. (2002). A lesion of the posterior parietal cortex disrupts on-line adjustments during aiming movements. *Neuropsychologia, 40*(13), 2471–2480.
Grill-Spector, K., Kushnir, T., Edelman, S., Itzchak, Y., & Malach, R. (1998). Cue-invariant activation in object-related areas of the human occipital lobe. *Neuron, 21*(1), 191–202.
Grill-Spector, K., Kushnir, T., Hendler, T., & Malach, R. (2000). The dynamics of object-selective activation correlate with recognition performance in humans. *Nature Neuroscience, 3*(8), 837–843.
Hesse, C., Miller, L., & Buckingham, G. (2016). Visual information about object size and object position are retained differently in the visual brain: Evidence from grasping studies. *Neuropsychologia, 91*, 531–543.
Iacoboni, M., Koski, L. M., Brass, M., Bekkering, H., Woods, R. P., Dubeau, M. C., et al. (2001). Reafferent copies of imitated actions in the right superior temporal cortex. *Proceedings of the National Academy of Sciences USA, 98*(24), 13995–13999.
Jackson, S. R., & Shaw, A. (2000). The Ponzo illusion affects grip-force but not grip-aperture scaling during prehension movements. *Journal of Experimental Psychology: Human Perception and Performance, 26*(1), 418–423.
Jakobson, L. S., & Goodale, M. A. (1991). Factors affecting higher-order movement planning: A kinematic analysis of human prehension. *Experimental Brain Research, 86*(1), 199–208.
James, T. W., Humphrey, G. K., Gati, J. S., Menon, R. S., & Goodale, M. A. (2002). Differential effects of viewpoint on object-driven activation in dorsal and ventral streams. *Neuron, 35*(4), 793–801.
Jeannerod, M. (1984). The timing of natural prehension movements. *Journal of Motor Behavior, 16*(3), 235–254.
Jenmalm, P., Schmitz, C., Forssberg, H., & Ehrsson, H. H. (2006). Lighter or heavier than predicted: Neural correlates of corrective mechanisms during erroneously programmed lifts. *The Journal of Neuroscience, 26*(35), 9015–9021.
Kentridge, R. W. (2014). Object perception: Where do we see the weight? *Current Biology, 24*(16), R740–R741.
Konen, C. S., & Kastner, S. (2008). Two hierarchically organized neural systems for object information in human visual cortex. *Nature Neuroscience, 11*(2), 224–231.
de Lange, F. P. (2006). Weight lifting in the human brain. *The Journal of Neuroscience, 26*(41), 10327–10328.
Lee Masson, H., Wallraven, C., & Petit, L. (2017). "Can touch this": Cross-modal shape categorization performance is associated with microstructural characteristics of white matter association pathways. *Human Brain Mapping, 38*(2), 842–854.
Leemans, A., Jeurissen, B., Sijbers, J., & Jones, D. K. (2009). ExploreDTI: A graphical toolbox for processing, analyzing, and visualizing diffusion MR data. In *17th Annual Meeting of Intl Soc Mag Reson Med Hawaii, USA* (p. 3537).
Lemon, R. N., Johansson, R. S., & Westling, G. (1995). Corticospinal control during reach, grasp, and precision lift in man. *The Journal of Neuroscience, 15*(9), 6145–6156.

Lukos, J. R., Ansuini, C., & Santello, M. (2007). Choice of contact points during multidigit grasping: Effect of predictability of object center of mass location. *The Journal of Neuroscience, 27*(14), 3894–3903.
Mahon, B. Z., Kumar, N., & Almeida, J. (2013). Spatial frequency tuning reveals interactions between the dorsal and ventral visual systems. *Journal of Cognitive Neuroscience, 25*(6), 862–871.
Malach, R., Reppas, J. B., Benson, R. R., Kwong, K. K., Jiang, H., Kennedy, W. A., et al. (1995). Object-related activity revealed by functional magnetic resonance imaging in human occipital cortex. *Proceedings of the National Academy of Sciences of the USA, 92*(18), 8135–8139.
Martin, M., Beume, L., Kümmerer, D., Schmidt, C. S., Bormann, T., Dressing, A., et al. (2016). Differential roles of ventral and dorsal streams for conceptual and production-related components of tool use in acute stroke patients. *Cerebral Cortex, 26*(9), 3754–3771.
McKeefry, D. J., & Zeki, S. (1997). The position and topography of the human colour centre as revealed by functional magnetic resonance imaging. *Brain, 120*(Pt 12), 2229–2242.
Merriam, E. P., Gardner, J. L., Movshon, J. A., & Heeger, D. J. (2013). Modulation of visual responses by gaze direction in human visual cortex. *The Journal of Neuroscience, 33*(24), 9879–9889.
Milner, A. D. (1997). Vision without knowledge. *Philosophical Transactions of the Royal Society of London B Biological Sciences, 352*(1358), 1249–1256.
Milner, A. D. (2017). How do the two visual streams interact with each other? *Experimental Brain Research, 235*, 1297–1308.
Milner, A. D., & Goodale, M. A. (2008). Two visual systems re-viewed. *Neuropsychologia, 46*(3), 774–785.
Monaco, S., Chen, Y., Medendorp, W. P., Crawford, J. D., Fiehler, K., & Henriques, D. Y. (2014). Functional magnetic resonance imaging adaptation reveals the cortical networks for processing grasp-relevant object properties. *Cerebral Cortex, 24*(6), 1540–1554.
Nowak, D. A., Glasauer, S., & Hermsdörfer, J. (2013). Force control in object manipulation-A model for the study of sensorimotor control strategies. *Neuroscience and Biobehavioral Reviews, 37*(8), 1578–1586.
Oldfield, R. C. (1971). The assessment and analysis of handedness: The Edinburgh inventory. *Neuropsychologia, 9*(1), 97–113.
Oosterhof, N. N., Wiggett, A. J., Diedrichsen, J., Tipper, S. P., & Downing, P. E. (2010). Surface-based information mapping reveals crossmodal vision-action representations in human parietal and occipitotemporal cortex. *Journal of Neurophysiology, 104*(2), 1077–1089.
Oram, M. W., & Perrett, D. I. (1996). Integration of form and motion in the anterior superior temporal polysensory area (STPa) of the macaque monkey. *Journal of Neurophysiology, 76*(1), 109–129.
Paulignan, Y., Jeannerod, M., MacKenzie, C., & Marteniuk, R. (1991). Selective perturbation of visual input during prehension movements. 2. The effects of changing object size. *Experimental Brain Research, 87*(2), 407–420.
Paulignan, Y., MacKenzie, C., Marteniuk, R., & Jeannerod, M. (1990). The coupling of arm and finger movements during prehension. *Experimental Brain Research, 79*(2), 431–435.
Peelen, M. V., & Caramazza, A. (2012). Conceptual object representations in human anterior temporal cortex. *The Journal of Neuroscience, 32*(45), 15728–15736.
Pisella, L., Gréa, H., Tilikete, C., Vighetto, A., Desmurget, M., Rode, G., et al. (2000). An 'automatic pilot' for the hand in human posterior parietal cortex: Toward reinterpreting optic ataxia. *Nature Neuroscience, 3*(7), 729–736.
van Polanen, V., & Davare, M. (2015). Interactions between dorsal and ventral streams for controlling skilled grasp. *Neuropsychologia, 79*(Pt B), 186–191.
Prado, J., Clavagnier, S., Otzenberger, H., Scheiber, C., Kennedy, H., & Perenin, M. T. (2005). Two cortical systems for reaching in central and peripheral vision. *Neuron, 48*(5), 849–858.
Ramayya, A. G., Glasser, M. F., & Rilling, J. K. (2010). A DTI investigation of neural substrates supporting tool use. *Cerebral Cortex, 20*(3), 507–516.
Rice, N. J., Tunik, E., & Grafton, S. T. (2006). The anterior intraparietal sulcus mediates grasp execution, independent or requirement to update: New insights from transcranial magnetic stimulation. *The Journal of Neuroscience, 26*(31), 8176–8182.
Rizzolatti, G., & Matelli, M. (2003). Two different streams form the dorsal visual system: Anatomy and functions. *Experimental Brain Research, 153*(2), 146–157.
Ross, E. D. (2008). Sensory-specific amnesia and hypoemotionality in humans and monkeys: Gateway for developing a hodology of memory. *Cortex, 44*, 1010–1022.
Rossetti, Y., Revol, P., McIntosh, R., Pisella, L., Rode, G., Danckert, J., et al. (2005). Visually guided reaching: Bilateral posterior parietal lesions cause a switch from fast visuomotor to slow cognitive control. *Neuropsychologia, 43*(2), 162–177.
Roth, Z. N., & Zohary, E. (2015). Position and indentity information available in fMRI patterns of activity in human visual cortex. *The Journal of Neuroscience, 35*(33), 11559–11571.
Schenk, T. (2012). No dissociation between perception and action in patient DF when haptic feedback is withdrawn. *The Journal of Neuroscience, 32*(6), 2013–2017.
Schenk, T., & McIntosh, R. D. (2009). Do we have independent visual streams for perception and action? *Cognitive Neuroscience, 1*(1), 52–62.
Schmitz, C., Jenmalm, P., Ehrsson, H. H., & Forssberg, H. (2005). Brain activity during predictable and unpredictable weight changes when lifting objects. *Journal of Neurophysiology, 93*(3), 1498–1509.
Schroeder, C. E., Mehta, A. D., & Givre, S. J. (1998). A spatiotemporal profile of visual system activation revealed by current source density analysis in the awake macaque. *Cerebral Cortex, 8*(7), 575–592.
Shapiro, K., Hillstrom, A. P., & Husain, M. (2002). Control of visuotemporal attention by inferior parietal and superior temporal cortex. *Current Biology, 12*(15), 1320–1325.
Shapiro, S. S., & Wilk, M. B. (1965). Analysis of variance test for normality (complete samples). *Biometrika, 52*(3/4), 591–611.
Sim, E. J., Helbig, H. B., Graf, M., & Kiefer, M. (2015). When action observation facilitates visual perception: Activation in visuo-motor areas contributes to object recognition. *Cerebral Cortex, 25*(9), 2907–2918.
Singh-Curry, V., & Husain, M. (2009). The functional role of the inferior parietal lobe in the dorsal and ventral stream dichotomy. *Neuropsychologia, 47*(6), 1434–1448.
Takemura, H., Rokem, A., Winawer, J., Yeatman, J. D., Wandell, B. A., & Pestilli, F. (2016). A major human white matter pathway between dorsal and ventral visual cortex. *Cerebral Cortex, 26*(5), 2205–2214.
Thiebaut de Schotten, M., Cohen, L., Amemiya, E., Braga, L. W., & Dehaene, S. (2014). Learning to read improves the structure of the arcuate fasciculus. *Cerebral Cortex, 24*(4), 989–995.
Tootell, R. B., Mendola, J. D., Hadjikhani, N. K., Ledden, P. J., Liu, A. K., Reppas, J. B., et al. (1997). Functional analysis of V3A and related areas in human visual cortex. *The Journal of Neuroscience, 17*(18), 7060–7078.
Tournier, J. D., Calamante, F., & Connelly, A. (2007). Robust determination of the fibre orientation distribution in diffusion MRI: Non-negativity constrained super-resolved spherical deconvolution. *Neuroimage, 35*(4), 1459–1472.
Tournier, J. D., Calamante, F., Gadian, D. G., & Connelly, A. (2004). Direct estimation of the fiber orientation density function from diffusion-weighted MRI data using spherical deconvolution. *Neuroimage, 23*(3), 1176–1185.

Tunik, E., Frey, S. H., & Grafton, S. T. (2005). Virtual lesions of the anterior intraparietal area disrupt goal-dependent on-line adjustments of grasp. *Nature Neuroscience, 8*(4), 505–511.

Ungerleider, L. G., Galkin, T. W., Desimone, R., & Gattass, R. (2008). Cortical connections of area V4 in the macaque. *Cerebral Cortex, 18*(3), 477–499.

Ungerleider, L. G., & Mishkin, M. (1982). Two cortical visual systems. In D. J. Ingle, M. A. Goodale, & R. J. W. Mansfield (Eds.), *Analysis of visual behavior* (pp. 549–586). Cambridge, MA: MIT Press.

Vinberg, J., & Grill-Spector, K. (2008). Representation of shapes, edges, and surfaces across multiple cues in the human visual cortex. *Journal of Neurophysiology, 99*(3), 1380–1393.

Wade, A. R., Brewer, A. A., Rieger, J. W., & Wandell, B. A. (2002). Functional measurements of human ventral occipital cortex: Retinotopy and colour. *Philosophical Transactions of the Royal Society of London B Biological Sciences, 357*(1424), 963–973.

Wang, R., Benner, T., Sorensen, A. G., & Wedeen, V. J. (2007). Diffusion toolkit: A software package for diffusion imaging data processing and tractography. *Proceedings of the International Society for Magnetic Resonance in Medicine, 15*, 3720.

Weiner, K. S., Yeatman, J. D., & Wandell, B. A. (2016). The posterior arcuate fasciculus and the vertical occipital fasciculus. *Cortex*. https://doi.org/10.1016/j.cortex.2016.03.012.

Wing, A. M., Turton, A., & Fraser, C. (1986). Grasp size and accuracy of approach in reaching. *Journal of Motor Behavior, 18*(3), 245–260.

Yeatman, J. D., Rauschecker, A. M., & Wandell, B. A. (2013). Anatomy of the visual word form area: Adjacent cortical circuits and long-range white matter connections. *Brain and Language, 125*(2), 146–155.

Yeatman, J. D., Weiner, K. S., Pestilli, F., Rokem, A., Mezer, A., & Wandell, B. A. (2014). The vertical occipital fasciculus: A century of controversy resolved by in vivo measurements. *Proceedings of the National Academy of Sciences U S A, 111*(48), E5214–E5223.

Zeki, S., Watson, J. D., Lueck, C. J., Friston, K. J., Kennard, C., & Frackowiak, R. S. (1991). A direct demonstration of functional specialization in human visual cortex. *The Journal of Neuroscience, 11*(3), 641–649.

Zhong, Y. M., & Rockland, K. S. (2003). Inferior parietal lobule projections to anterior inferotemporal cortex (area TE) in macaque monkey. *Cerebral Cortex, 13*(5), 527–540.

Zimmermann, M., Verhagen, L., de Lange, F. P., & Toni, I. (2016). The extrastriate body area Computes Desired goal states during action planning. *eNeuro, 3*(2). https://doi.org/10.1523/ENEURO.0020-16.2016.